Hyperfine Interactions (2021) 242: 12
https://doi.org/10.1007/s10751-021-01741-7

Velocity waveform digitalization for quality control and enhancement of Mössbauer effect spectra acquisition

Gustavo A. Pasquevich[1,2,3] · **Alejandro L. Veiga**[3,4]

Accepted: 5 October 2021 / Published online: 21 October 2021

Abstract
The Error and Monitor signals of the Mössbauer driver can be used to infer the true velocity in the acquisition of a Mössbauer spectrum. This information can be recorded to substantially improve the collected data. It can be used to perform quality control of the spectra, validate regions of good linearity and correct non-linearities. In particular the error waveform is essential to account for possible deviations of the channel-to-velocity relation from the expected one. These deviations are mainly due to the physical limitations of the feedback control system. They are almost impossible to anticipate and they vary considerably when modifying the amplitude or shape of the velocity reference, or when modifying the parameters of the closed-loop control system. The sampling of the Error and Monitor waveforms can be carried out with a standard digital oscilloscope, while maintaining a correct synchronization and resolution, necessary for a correct post-analysis. In this paper a method for wave acquisition and reconstruction is proposed. The effects of non-controlled oscillations at the abrupt changes of velocity variation in alpha Fe spectra are discussed. It is also shown how the acquisition can be performed remotely and automatically, without disturbing the measurement or decreasing the efficiency of the spectrometer.

Keywords Mössbauer effect spectroscopy · Velocity · Calibration · Remote control

Gustavo A. Pasquevich and Alejandro L. Veiga contributed equally to this work.

This article is part of the Topical Collection on *Proceedings of the International Conference on the Applications of the Mössbauer Effect (ICAME 2021), 5-10 September 2021, Brasov, Romania*
Edited by Victor Kuncser

✉ Gustavo A. Pasquevich
gpasquev@fisica.unlp.edu.ar

Alejandro L. Veiga
alejandro.veiga@ing.unlp.edu.ar

[1] Instituto de Física La Plata, CONICET, La Plata, Argentina

[2] Dto. de Física, Facultad de Ciencias Exactas, Universidad Nacional de La Plata, La Plata, Argentina

[3] Facultad de Ingeniería, Universidad Nacional de La Plata, La Plata, Argentina

[4] Instituto de Investigaciones en Electrónica, Control y Procesamiento de Señales (LEICI-CONICET), La Plata, Argentina

1 Introduction

Nowadays, due to the restrictions caused by the COVID19 pandemic, access to laboratories has been considerably reduced. Therefore, it has been an increase in search for strategies that enable the remote use of the equipment. Even prior to the pandemic, access to many laboratories was limited due to institutional policies. For example, the closure of activities during nights, weekends and recess periods. For laboratories using radioactive sources, these policies or constraints are counterproductive, implying irretrievable loss of use of radioactive sources. In this sense, it is necessary to manage the time of use of the spectrometer in an efficient way and try to operate even during these periods [1]. On the other hand, Mössbauer spectroscopy experiments are slow experiments and therefore convenient to be controlled remotely [2].

Modification of the maximum velocity of the spectrum is one of the aspects of spectroscopy that often requires in person attendance. When velocity range is modified, it is recommended to perform a new spectrometer calibration [3] (e.g. acquisition of an α-Fe spectrum). The velocity range change is usually defined in advance. However, the need for this change may arise during the acquisition of a spectrum, for example, when unexpected presence or absence of spectral components is detected. In this sense, multi-sample holders [2, 3] (making sure that they carry a calibration sample) are a good solution for remote calibration. However, they are not useful for experiments using furnaces, cryostats or any other equipment not compatible.

A good knowledge of the velocity-channel relationship is essential to ensure good spectrum quality. However, non-linearities in this relationship [4, 5] (mainly due to control limitations) make difficult the achievement of this goal.

The Mössbauer effect spectrum is obtained by moving the radioactive source (or absorber) by means of an electromagnetic velocity transducer following a defined reference waveform. The Mössbauer velocity transducers are based on the principle of two coupled loudspeakers. A drive coil causes the motion of the transducing element and a pickup coil returns a signal proportional to velocity to the Driver unit [3, 6]. This signal is well representing the velocity with non-linearities less than 0.15% [6, 7]. Figure 1 shows a diagram of the operation of the Mössbauer driver and the velocity transducer. The Driver, by means of a feedback control with feed-forward and PID compensations, acts on the drive coil and tries to make the pickup signal copy the Monitor signal (proportional to the Reference signal). The Driver (usually) provides two monitoring outputs, the Monitor signal and the Error signal, proportional to the difference between the Monitor signal and the Pickup signal, as shown in Fig. 1 [6, 8, 9].

The true velocity of the source (or absorber) is proportional to the pickup signal, and can be expressed from the Monitor and Error signals,

$$v = \alpha_0 V_{pickup} = \alpha_0 \left(V_{Monitor} + \alpha_1 V_{Error} \right) \tag{1}$$

where α_0 and α_1 are two factors that depend on the transducer and driver electronics. For the case of the WissEl MVT1000 transducer and CMTE-Halder MR350 driver, these factors are approximately 25 mm/s/V and 0.01 respectively [6, 7]. Usually the Monitor signal is a well known signal (proportional to the reference input of the drive), while the pickup and error signals cannot be accurately anticipated. From these, the Error signal is easier to record due to its lower dynamic range. The precise values of α_0 and α_1, required to calibrate the driver and velocity transducer assembly, can be obtained by recording a calibration Mössbauer effect spectrum (e.g. α-Fe), and the corresponding Monitor and Error signals.

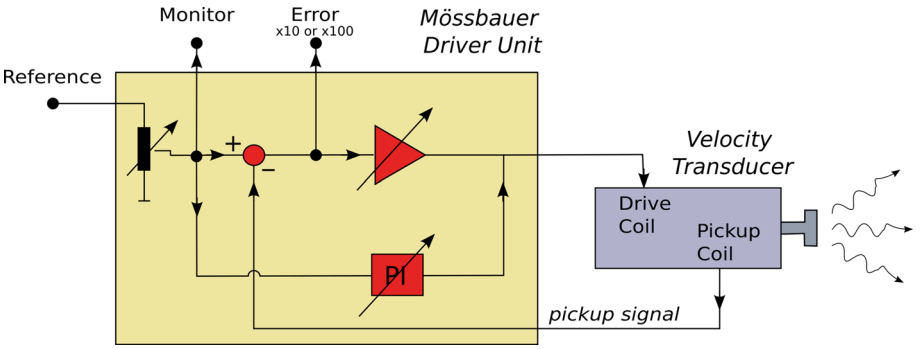

Fig. 1 Block diagram of the Mössbauer Driver Unit and the Velocity Transducer

With the real velocity of the transducer corresponding to each channel of the spectrum it is possible to discuss the quality of the spectra, to validate regions of good linearity or even to correct existing non-linearities. It can also be used to calibrate a spectrometer after a reference change without the requirement of a new calibration spectrum. In order to record the Monitor and Error waveforms it is necessary to use an analog-to-digital converter (ADC) of more than 12 bits (see Section 3) with a high sampling rate. A digital oscilloscope is a tool that can be used for sampling purposes. However, many standard digital oscilloscopes do not have resolutions greater than 8 or 9 bits.

Both signals have the advantage of being periodic. This allows the use of averaging techniques of the oscilloscope (if available) to improve the resolution of the digitization [10]. This same feature allows to exploit the flexibility of the oscilloscope input range (V/div) to sample the signals by zones and then, by means of an appropriate algorithm, reconstruct the complete waveforms.

In this work we propose the partial sampling and full-wave reconstruction algorithms. With the recorded waves we reconstruct the true velocity wave, finding the α_0 and α_1 factors of the equipment. Finally we discuss the advantages of incorporating this information in the acquisition of a spectrum.

2 Experimental

A transmission geometry spectrometer was used to record the spectra, using a WissEl MVT1000 velocity transducer, a Mössbauer CMTE MR350 driver, and a multichannel scaler with a programmable waveform generator (MDAQ107 [11]). The detection branch consists of an LND-4546 proportional counter detector and ORTEC electronics (pre-amplification, amplification and single channel analyzer). The MR350 driver provides the two required outputs, Monitor and Error, being the last one the difference (x100) between the pickup signal and the reference signal, as shown in Fig. 1.

The Monitor and Error waveforms were sampled with a TekTronix TDS3012 oscilloscope (100MHz 1.25GS/s) equipped with TDS3GV communication module. The sampling algorithm was programmed in Python using the PySerial package [12].

Spectra were taken using a 12 μm α-Fe foil and a ^{57}Co(Rh) source of 50 mCi. The distance between the source and the detector was approximately 19 cm. The frequency of the triangular wave was set at 26 Hz. Changes on reference amplitude (maximum velocity) were performed using MDAQ107 internal gain.

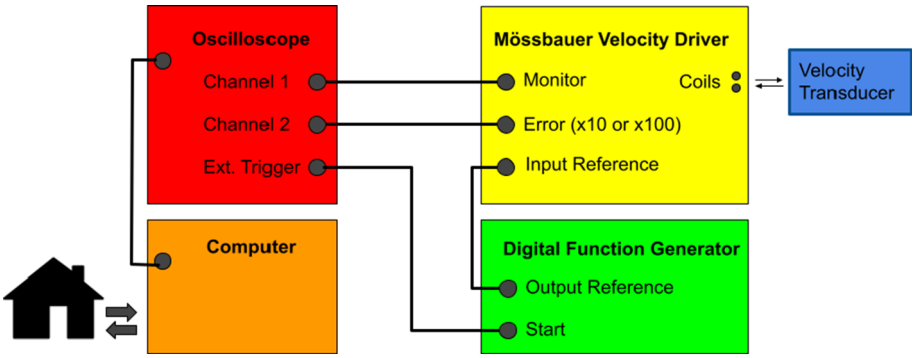

Fig. 2 Configuration used for waveform sampling

3 Sampling and reconstruction algorithms

Between the two waveforms to be sampled, the most demanding is the Monitor, due to its large dynamic range. This waveform must be sampled at a considerably higher resolution than $\frac{N_{ch}}{2}$ (where N_{ch} is the number of channels of the multichannel scaler). If we intend to sample n_{ptc} points per channel, for full sampling we need an $n_{need} = \log_2\left(\frac{1}{2}N_{ch}n_{ptc}\right)$ bit converter. Note that if you want to sample a full 1024 channel waveform with at least 5 points per channel you need a converter of at least 12 bits. But if the ADC has a resolution of n_{adc} bits ($< n_{need}$), it can only be used to sample a fraction of the signal with the desired resolution. This fraction corresponds to a range $\Delta V = \frac{2V_{pp}2^{n_{adc}}}{N_{ch}n_{ptc}}$, where V_{pp} is the peak to peak amplitude. This range and the frequency of the wave f define the optimal time window to take full advantage of the vertical scale, $\Delta T = \frac{n_{adc}}{fN_{ch}n_{ptc}}$. With these values determined, a sampling algorithm can be proposed to collect the full waveform values.

The Error waveform has less dynamic range requirements. It is a signal that, in the region where the generated waveform is well controlled by the driver, has a variation range around a fraction of channels. Therefore the 8-bit resolution of the oscilloscope is enough for sampling the signal in this region. Vertical scale should be selected avoiding saturation.

To synchronize the sampling of both waveforms with the multichannel scaler, the configuration presented in Fig. 2 is proposed. The oscilloscope is configured to be triggered by an external signal for which the START output of the Digital Function Generator is used. The Monitor and Error outputs are recorded with two oscilloscope channels. This configuration can remain mounted during the spectrum acquisition and waveform sampling can be performed remotely, as many times as required.

The sequential sampling algorithm (Fig. 3) chooses the next window position based on the previous sampling. Acquisitions are performed using the average of n_{avg} cycles provided by the oscilloscope (in this work n_{avg}= 128). The windows are specified by indicating the center of the window (in time and voltage). The values are referred to t=0 (defined by the trigger) and V=0 (GND). The delay and offset controls of the oscilloscope are used to define the window positions. The error signal does not require an offset and can be sampled by keeping the window at V=0. However, in areas of abrupt velocity change, there may be overshoot (or undershoot) that can saturate the signal. When this happens, sampling is repeated by increasing the amplification (vertical scale) until a sampling without saturation is achieved. In this algorithm, a factor of 10 was chosen for scale increases. The sampling

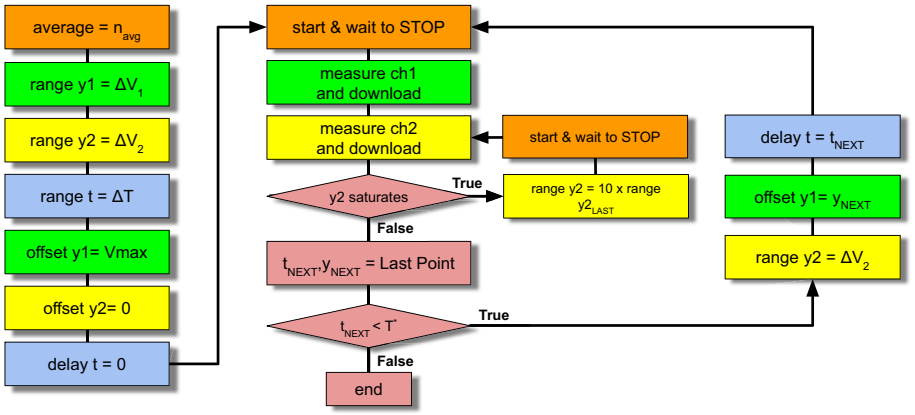

Fig. 3 Flowchart of the acquisition algorithm used for the sampling of the Monitor and Error waveform of the Mössbauer driver. Here, y1 corresponds to the voltage signal in channel 1 where the reference signal (Monitor) is recorded and y2 corresponds to channel 2 (Error). The following color code is used: orange for general operations on the oscilloscope. green for channel 1 (Monitor waveform), yellow for channel 2 (Error waveform), blue for time scale, and red for operations specific to the algorithm

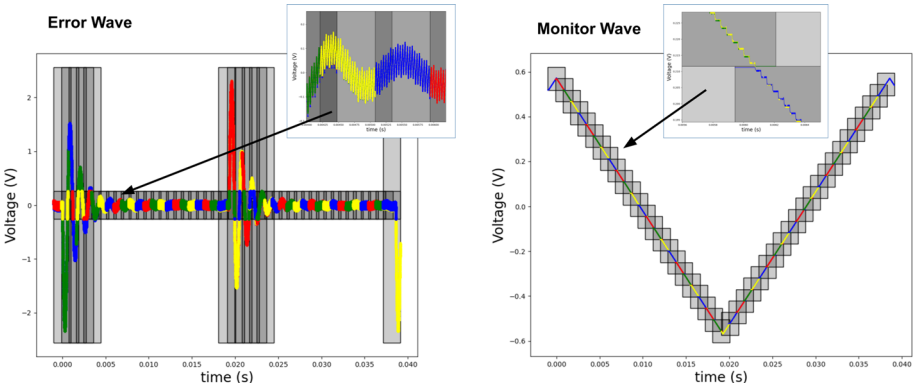

Fig. 4 Set of recorded waveform sections, sequentially colored with 4 different colors. Gray translucent boxes indicate the size and position of the selected windows

of the Monitor signal defines the position of the next window, which is positioned at the center of the last unsaturated point that was recorded in the previous sampling (t_{NEXT} and $y2_{NEXT}$ in Fig. 3). All measurements are saved on the PC in different files. Figure 4 shows the fractions collected for both waves, identifying the windows selected for each sampling.

All these measurements are performed simultaneously and without affecting the spectrum acquisition. The acquisition time depends on the communication technology between the PC and the oscilloscope. In this work, 38400 baud rate serial communication was available, resulting in a net time of about 25 minutes for a complete recording of the whole waveforms set. This time can be considerably reduced if higher bandwidth communication technologies are used.

A python script is used to reconstruct the Monitor and Error waves from the set of collected partial samples. The waves are averaged where they overlap. In the case of Error

waves, where larger scale samples appear, the averaging is done with weight inversely proportional to the scale used. This process results in two data sets for the complete period of both waves.

The synchronization between waves and channel sweep is based on the determination of the wave period and initial and final positions of the triangular waveform. For this purpose, a triangle of period T is fitted, from which T, t_0 and t_{end} are obtained. Channel positions are regularly distributed within the interval [t_0,t_{end}]. This distribution depends on the correlation between triangular reference wave and channel position, defined by digital function generator and multichannel scaler. In this case, we use non-commercial MDAQ107 equipment (with versatility in waveform definition [11]). A triangular wave with well-defined edges was chosen, defined by the values $[-v_m + \frac{2i}{N_{ch}} v_m, i = 0, 1, 2, \frac{N_{ch}}{2} - 1] + [v_m - \frac{2i}{N_{ch}} v_m, i = 0, 1, 2, \frac{N_{ch}}{2} - 1]$, where v_m is maximum velocity (or voltage).

4 Results

The availability of Monitor and Error waves can substantially improve the quality of the acquired spectra. We now show how the inferred velocity waveform is consistent with the recorded spectrum, even when the absorption lines are close to the triangular wave peaks and distorted for this reason. For this purpose, an α-Fe spectrum was recorded using a triangular wave, in a velocity range of ± 6 mm/s and ± 8 mm/s. Simultaneously, the Error and Monitor waves are recorded.

Since the relation between channel and voltage signals is available and the functional dependence between these signals and the velocity is known (Eq. 1), the counts in the multichannel scaler should follow this expression,

$$y(v) = r_0(t, x_0, T, \varphi) \left[1 - \sum_{i=1}^{6} h_i \frac{\Gamma_i^2}{4} \frac{1}{\left(\frac{\Gamma_i}{2}\right)^2 + (v - \delta - c_i B_0)^2} \right] \tag{2}$$

where

$$v(t) = \alpha_0 \left[\mathbf{Mon}\,(t - \varphi) + \alpha_1\, \mathbf{Err}\,(t - \varphi) \right] \tag{3}$$

and φ is the phase shift between the measured waves (Monitor and Error) and the channel sweep. In Eq. 2, $r_0(t, x_0, T, \varphi)$ is the count at the baseline, taking into account the dependence on changes in solid angle during source motion, x_0 and T are the source detector mean distance and wave period respectively. In the same equation, c_i are the proportional factors between the ^{57}Fe magnetic hyperfine field and the position of the six absorption lines relative to the isomeric shift [3]. Being $c_1 = c_6 = 1$, $c_2 = c_5 = 0.5790$ and $c_3 = c_4 = 0.1581$. B_0 is half distance between external lines in α-Fe at room temperature, 5.31 mm/s. Parameter δ is the isomer shift, and h_i and Γ_i are absorption lines depth and FWHM respectively, taken both symmetrically equal: $h_1 = h_6$, $h_2 = h_5$, $h_3 = h_4$, $\Gamma_1 = \Gamma_6$, $\Gamma_2 = \Gamma_5$ and $\Gamma_3 = \Gamma_4$.

Figure 5 shows the spectra recorded with the triangular waveform and the fitted curve using Eqs. 2 and 3. Table 1 shows the parameters resulting from the fitting analysis. Note in the figure that the spectrum recorded at ± 6 mm/s is clearly affected by the oscillations in velocity that occur at the abrupt change of acceleration. In the case of the spectrum at ± 8 mm/s these oscillations also occur, but they are not so evident in the spectrum lines, which are now farther away from the triangular edges. It is worth noting that despite the clear differences between the two spectra, the adjusted parameters were almost the same

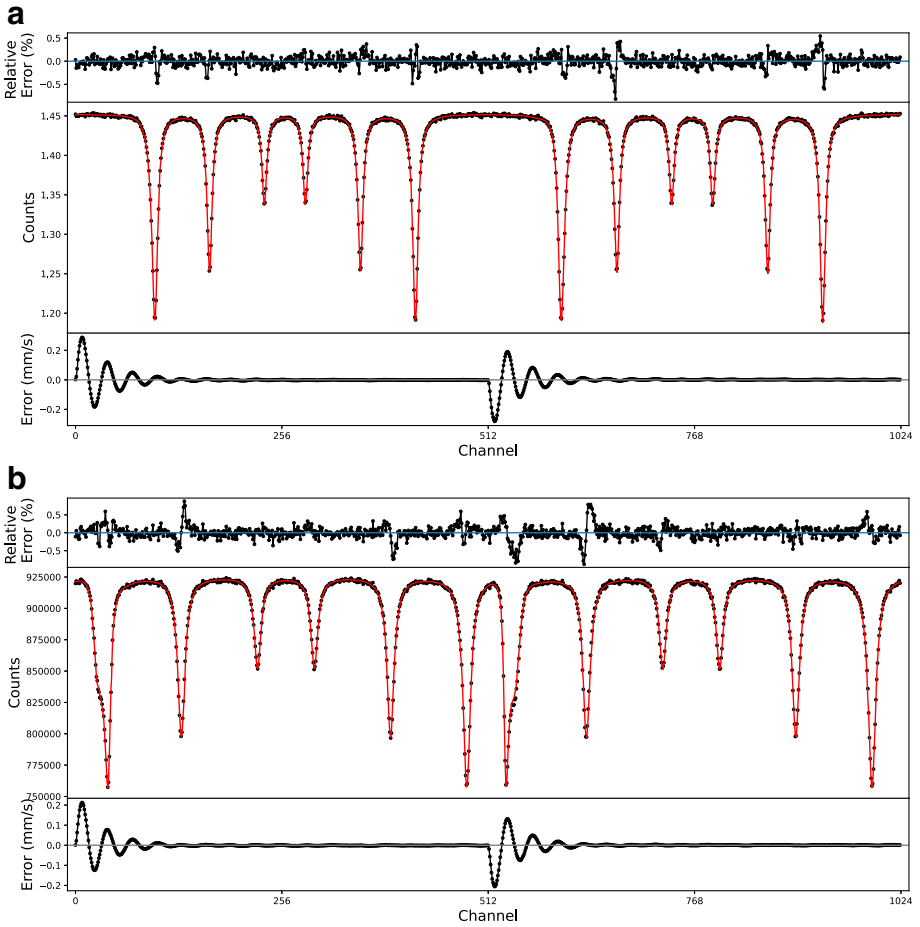

Fig. 5 Spectra recorded with a triangular waveform programmed on the MDAQ107 multichannel scaler, using 1024 channels. The full red line shows the fitting curve considering the α-Fe absorption spectrum and the reconstructed velocity from the Monitor and Error waveforms of the Mössbauer driver. The upper plot of each figure shows the porcentual difference between the fit and the spectrum. The lower plot shows the acquired Error waveform (multiplied by the parameters α_0 and α_1 to be presented in mm/s). a) Results of the experiment performed with a peak-to-peak velocity of ∼8 mm/s. b) Spectrum taken with a peak-to-peak velocity of ∼6 mm/s

Table 1 Fitting parameters using Eqs. 2 and 3 over two unfolded spectra taken with triangular waves of different amplitudes. Last column is reduced chi square

Spectrum	α_0 [mm/s]	α_1	φ [channels]	δ [mm/s]	Γ_1 [mm/s]	Γ_2 [mm/s]	Γ_3 [mm/s]	red-χ^2
±8 mm/s	24.018(1)	-0.0087(2)	0.356(5)	−0.1095(2)	0.2615(7)	0.2466(9)	0.240(2)	2.1
±6 mm/s	24.039(1)	-0.0088(1)	0.343(9)	−0.1092(2)	0.254(1)	0.249(1)	0.243(2)	3.0

regardless of the speed range chosen. The values of α_0 and α_1 turn out to be very similar for both spectra, and their values are consistent with the approximate values reported by the manufacturer. [6, 7] The same is true for the spectral parameters: isomeric shift of the α-Fe and linewidths. These results indicate that the velocity-to-channel relation is correctly expressed by Eqs. 1 and 3, and that the parameters α_0 and α_1 are determinable from the measurement of a well known spectrum and the Monitor and Error waveforms of the Driver Unit.

5 Conclusions

It is possible to digitalize the Monitor and Error waveforms that define the movement of the source and reconstruct its real velocity. Sampling can be performed with a digital oscilloscope with communications, usually available in laboratories. This sampling can be performed remotely and can be done as many times as necessary, without interfering with the acquisition of the spectra. The recorded waveforms can be used to confirm the correct operation of the equipment, to check good linearity regions of the multichannel scaler and to correct non-linearities that arise due to the limitations of the feedback control.

Acknowledgments The financial support for this work was granted by Agencia Nacional de Promoción de la Investigación, el Desarrollo Tecnológico y la Innovación (ANPCyT) and Consejo Nacional de Investigaciones Científicas y Técnicas (CONICET) of Argentina, with projects, PICT 2017-1748 and PUE 22920170100066CO respectively.

References

1. López, J.H., Restrepo, J., Barrero, C.A., Tobón, J.E., Ramírez, L.F., Jaramillo, J.: Autonomous sample switcher for Mössbauer spectroscopy. Hyperfine Interactions 238(1). https://doi.org/10.1007/s10751-017-1424-8 (2017)
2. Silaev, A.A., Godovikov, S.K., Postnikov, E.B., Radchenko, V.V., Silaev, A.A.: Remote access Mössbauer spectrometry. Bulletin of the Russian Academy of Sciences: Physics **77**(6), 790–794 (2013). https://doi.org/10.3103/s1062873813060324
3. Gütlich, P., Bill, E., Trautwein, A.X.: Mössbauer Spectroscopy and Transition Metal Chemistry. Springer, New York (2011). https://doi.org/10.1007/978-3-540-88428-6
4. Spiering, H., Nagy, D.L., Németh, Z., Bogdán, C., Deák, L.: Non-linearity correction of the velocity scale of a Mössbauer spectrum. Nuclear Instruments and Methods in Physics Research Section B: Beam Interactions with Materials and Atoms **480**, 98–104 (2020). https://doi.org/10.1016/j.nimb.2020.06.048
5. Kohout, P., Pechoušek, J., Kouřil, L.: Evaluation of Mössbauer spectra linearization methods. Hyperfine Interactions 240(1). https://doi.org/10.1007/s10751-019-1667-7 (2019)
6. Fast ComTec Gmbh: Operating Manual Mössbauer Driver Systems 351 MA-250/MR351
7. WissEl - Wissenschaftliche Elektronik GmbH: Operating Manual Mössbauer Velocity Transducer MVT1000
8. WissEl - Wissenschaftliche Elektronik GmbH: Operating Manual Mössbauer Driver Unit MR360
9. WissEl - Wissenschaftliche Elektronik GmbH: Operating Manual Mössbauer Driver Unit MR260
10. TekTronix: Improving Vertical Resolution in Tektronix Digital Phosphor Oscilloscopes. Application Note (2013)
11. Veiga, A., Mayosky, M.A., Martínez, N., Mendoza Zélis, P., Pasquevich, G.A., Sánchez, F.H.: Smooth driving of Mössbauer electromechanical transducers. Hyperfine Interactions **202**(1-3), 107–115 (2011). https://doi.org/10.1007/s10751-011-0342-4
12. Liechti, C.: Pyserial package, Version 3.4. https://pyserial.readthedocs.io (2016)